

Ballistic Transport in 0.05 μm -Gate AlGaAs/GaAs MODFET

Tetsuzo Ueda, Keijiro Itakura, Kazuo Miyatsuji, Tsuyoshi Tanaka,
Daisuke Ueda, and *Chihiro Hamaguchi

Electronics Research Laboratory, Matsushita Electronics Corporation,
1-1 Saiwai-cho Takatsuki city, Osaka 569, Japan.

*Department of Electronic Engineering, Osaka University.
2-1 Yamada-Oka Suita City, Osaka 565, Japan.

We report for the first time an experimental evidence of ballistic transport in AlGaAs/GaAs MODFET with the gate length down to 0.05 μm . Based on the proposed modeling of the device, we have found that the carrier velocity of the device reaches $6.5 \times 10^7 \text{ cm/s}$ that is independent of temperature. This enhanced velocity is due to the high electric field under the gate, which is obtained by deep and narrow gate-recess process. The temperature-independency implies that the electrons are transported without suffering from optical phonon and/or inter-valley scattering.

1. Introduction

It has been recognized that nonstationary effects such as ballistic and overshoot carrier transport should improve the performance of deep-submicron demension devices. Recent advances of electron-beam lithography have enabled the fabrication of field effect transistors with deep-submicron gate lengths. Several reports have already been published on modulation-doped field effect transistors(MODFETs) with deep-submicron gate lengths that have shown excellent dc and microwave performance^{1,2)}. These performances would be attributed to the enhanced carrier velocity in the process of nonstationary transport. Although a lot of reports have been made on the ballistic transport in the MODFETs simulated by using Monte Carlo method³⁾, no experimental evidence of ballistic transport was obtained so far.

In this paper, we report for the first time the direct evidence of ballistic carrier transport in AlGaAs/GaAs MODFETs with the gate length down to 0.05 μm . The ballistic transport requires high electric field and very short carrier transit time under the gate. What is crucial in obtaining these features is to reduce the parastic resistance between source and drain and to reduce the gate length as well. Then we have reduced the parastic resistance by using 0.15 μm deep and 0.25 μm wide gate-recess. Based on the newly proposed modeling of the device, we extracted the carrier velocity in the devices from the dc characteristics at 77K and 300K. The velocity in the 0.05 μm -gate MODFET reaches $6.5 \times 10^7 \text{ cm/s}$ independent of temperatures.

shown in Fig.2, where the constant carrier velocity v_s is assumed under the gate. The depletion layer reaches just to the hetero-interface, then the current flows only in the 2DEG. First, we consider the long channel case as shown in Fig.2(a). The change of the current Δi in the 2DEG, which is modified by the change of the gate bias ΔV_g , is given by

$$\Delta i = \Delta Q v_s = C_{gs} v_s \Delta V_g \quad (1)$$

where ΔQ is the change of the charge under the gate and C_{gs} is the gate capacitance per unit area. Hence, the velocity is obtained by measured transconductance g_m per unit gate width and calculated C_{gs} , then

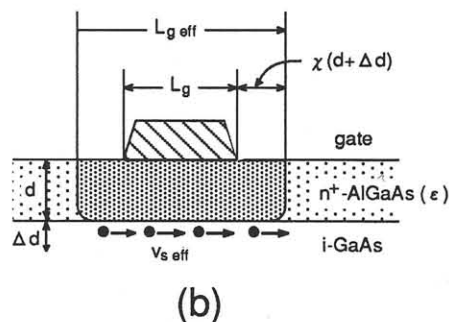
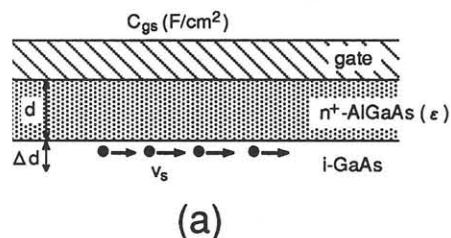


Fig.1 Schematic cross-section of the device modeling in the (a)long channel case, (b)short channel case.

2. Modeling for carrier velocities

Schematic cross section of our modeling is

$$v_s = \frac{g_m}{C_{gs}} \quad (2)$$

When the gate length decreases to submicron region, the effective gate length extended with the lateral depletion layer width must be considered. We estimate the effective gate length $L_{g\text{ eff}}$ introducing the widened ratio χ , then

$$L_{g\text{ eff}} = L_g + 2\chi(d+\Delta d) \quad (3)$$

where L_g is the gate length, d is the thickness of the AlGaAs layer and Δd is set-back distance in the 2DEG as shown in Fig.2(b). This gate fringing effect cause decreasing of C_{gs} by the ratio of $L_g/L_{g\text{ eff}}$. In this case, the C_{gs} in eq.(2) is given by

$$C_{gs} = \frac{\epsilon}{d+\Delta d} \frac{L_g}{L_{g\text{ eff}}} \quad (4)$$

where ϵ is the permittivity of the AlGaAs layer. From eq.(2) and (4), the effective carrier velocity $v_{s\text{ eff}}$ is extracted by using the following equation:

$$\begin{aligned} v_{s\text{ eff}} &= \frac{g_m(d+\Delta d)}{\epsilon} \frac{L_{g\text{ eff}}}{L_g} \\ &= \frac{g_m(d+\Delta d)}{\epsilon} \frac{L_g + 2\chi(d+\Delta d)}{L_g} \end{aligned} \quad (5)$$

3. Fabrication Process

The process for the 0.05 μm -gate MODFETs is as follows. The epi-structure is as shown in Fig.2, where the MBE grown AlGaAs/GaAs modulation-doped structure is seen. Planer isolation was employed using Boron implantation. AuGeNi/Au was evaporated and then alloyed to make ohmic contacts. After 0.25 μm gate-pattern of PMMA was opened by using electron beam lithography, $n^+\text{GaAs}$ contact layer was selectively etched by reactive ion etching using the gas mixture of $\text{CCl}_2\text{F}_2 + \text{He}$. The

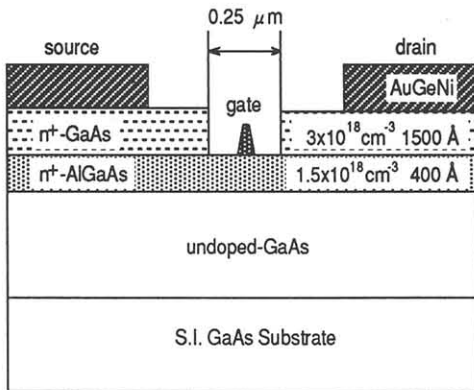


Fig.2 Schematic cross-section of the 0.05um-gate MODFET.

resultant gate-recess was formed 0.25 μm wide and 0.15 μm deep. 1500Å-thick Ti gate metal formed using electron-beam evaporation and lift-off process. Then it was thinned down to 0.05 μm of the gate length by exposing CF_4 plasma. The SEM cross section of the resultant device is shown in Fig.3. What is the most important in this process is a deep and narrow gate-recess to maintain high electric field under the gate.



Fig.3 SEM cross-section photograph of the 0.05 μm -gate MODFET.

4. Results and Discussion

The drain characteristics at 300K for the 0.05 μm -gate MODFET is shown in Fig.4. The maximum transconductance of the device with gate length ranging from 0.5 μm to 0.05 μm was measured at 77K and 300K. When the device shows the maximum transconductance, the depletion layer reaches to the 2DEG as assumed in the above mentioned modeling. The intrinsic transconductance $g_{m\text{ int}}$ was obtained from the maximum transconductance and the source resistance of the MODFET measured under those temperatures. Fig.5 is a plot of the obtained $g_{m\text{ int}}$ as a function of the gate length. It is noted in this figure is that the $g_{m\text{ int}}$ become independent of the temperature when the gate length decreases down to 0.05 μm .

The corresponding carrier velocity was also extracted from eq.(5). The velocities in the case of $\chi=1$ were plotted in Fig.6, where the velocity reaches the maximum value of $6.5 \times 10^7 \text{ cm/s}$ when the gate length decreases down to 0.05 μm . The obtained velocities are higher than the reported value of saturation drift velocity. The enhanced velocities are owing to the velocity overshoot effect. The fact that the velocity is independent of the temperature implies that the electrons are transported without suffering from optical phonon and/or inter-valley scattering. It is noted that the resultant temperature-independency has nothing to do with the value of χ in the modeling. This means the temperature-independency of the transconductance is the direct evidence of ballistic transport.

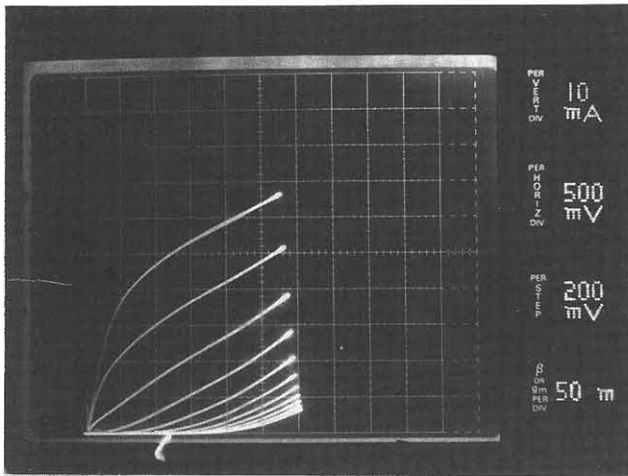


Fig.4 Current(I_d)-voltage(V_{ds}) characteristics for a $0.05\ \mu\text{m}$ -gate MODFET ($W_g=200\ \mu\text{m}$) at 300K.

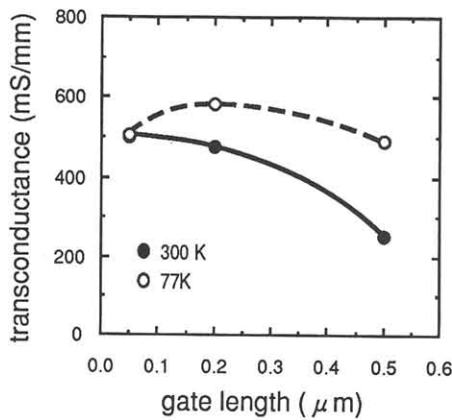


Fig.5 Transconductance at 77K and 300K as a function of gate length.

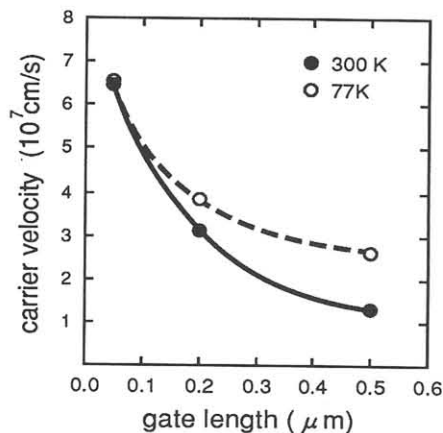


Fig.6 Carrier velocity at 77K and 300K as a function of gate length.

Since the measured source resistance per unit gate width of $0.05\ \mu\text{m}$ -gate MODFET is $1.2\ \Omega/\text{mm}$ and $0.4\ \Omega/\text{mm}$ at 300K and 77K, respectively, the electric field under the gate reaches $2.8 \times 10^5\ \text{V/cm}$ even at the temperature of 300 K. Thus obtained electric field is enough to achieve the ballistic transport effect.

The present result has good agreement with those reported so far obtained from Monte Carlo simulation⁴⁾.

5. Conclusion

Based on the proposed modeling of the device, we estimate that the carrier velocity in AlGaAs/GaAs MODFET with the gate length of $0.05\ \mu\text{m}$ reaches $6.5 \times 10^7\ \text{cm/s}$ independent of temperature. This fact implies that the electrons are transported without suffering from scatterings, which is a direct evidence of ballistic transport.

Acknowledgements

The authors would like to thank Dr.G.Kano and Mr.M.Kazumura for their encouragement in this work.

References

- 1) P.C.Chao, M.S.shur, R.C.Tiberio, K.H.G.Duh, P.M.Smith, J.M.Ballingall, P.Ho and A.A.Jabra: IEEE Trans. Electron Devices ED-36(1989)461.
- 2) L.D.Nguyen, L.M.Jelloian, M.Thompson and M.Lui: Int.Electron.Dev.Meeting 90 Tech.Dig., p499.
- 3) K.Yokoyama, M.Tomizawa and A.Yoshii: Extended Abstr. 18th Int.Conf.Solid State Devices and Materials, Tokyo, 1986, p339.
- 4) A.Ghis, E.Constant and B.Boittiaux: J.Appl.Phys. 54(1983)214.